Thermal neutron detection using boron-10 and sodium salicylate doped epoxy films

by

Hayn Park

Submitted to the Department of Physics
in partial fulfillment of the requirements for the degree of

Bachelor of Arts

at

HARVARD UNIVERSITY

June 1996

Author .....
Department of Physics
May 6, 1996

Certified by .....
John M. Doyle
Assistant Professor of Physics
Thesis Supervisor

Accepted by .....
Gary Feldman
Chairman, Department of Physics

Thermal neutron detection using boron-10 and sodium salicylate doped epoxy films

by

Hayn Park

Submitted to the Department of Physics
on May 6, 1996, in partial fulfillment of the
requirements for the degree of
Bachelor of Arts

Abstract

An epoxy-based neutron detecting film has been developed. Boric acid (H_3BO_3), 97% enriched in boron-10, and sodium salicylate (2-HOC_6H_4COONa) are mixed into a clear, colorless epoxy. Upon neutron capture by the boron-10 atom, an alpha particle (1.47 MeV), lithium-7 atom (0.84 MeV), and a gamma are produced. We believe the massive particles cause UV scintillations in the epoxy. Sodium salicylate, also present in the epoxy, downconverts the UV scintillations into visible light, which is detected by a photomultiplier tube.

We report the performance of these films in detecting thermal neutrons. We also report additional work on neutron detecting plastic films.

Thesis Supervisor: John M. Doyle
Title: Assistant Professor of Physics

Acknowledgments

I would like to thank the members of the Doyle research group for their advice, friendship, and delightfully rejuvenating lunch conversations.

I owe special thanks to Paul Huffman for his close help throughout the entire study, and all the sunny spring days at the nuclear reactor. I am indebted to John Doyle for his guidance and support, as well as his introducing me to a world of incredibly "neat things."

To Rick Goodman and Irfan Siddiqi, I owe valuable conversations on chemistry and techniques. I also send a warm thanks to Tom Newton and the crew at the MIT Nuclear Reactor Lab for their help, as well as to Wolfgang Rueckner and Joe Peidle closer to home at Harvard's Physics 191r lab.

And surely I haven't forgotten some of the most important people in my life: my parents, my sister, Arnico, Sandy, Brian, and all the other people who put up with my mysterious disappearances and one word replies. ("Sorry. Thesis.")

It has been quite an experience, and I'd do it all over again. Thank you all.

Contents

List of Figures

List of Tables

Chapter 1

Introduction

1.1 Epoxy and plastic-based detectors

Common detectors for thermal neutrons (0.025 eV) use BF_3 and ^3He, typically in large ionization chambers [1]. These ionization chambers may not be suited for experiments with cramped geometries, such as a recently proposed experiment to trap ultra-cold neutrons [2].

We have pursued the development of a clear, colorless, and easy-to-apply neutron detection film based on an epoxy resin or plastic doped with neutron converting compounds and UV downconverting compounds. We hypothesized that these two dopants in combination would capture incoming thermal neutrons and then emit pulses of visible light that could be detected by a photomultiplier tube (PMT).

The epoxies have a curing time of 8-16 hours; during this time, they can be shaped and poured into molds. Plastic films can be dissolved into a solvent, and the solution used for the same purpose. The plastic-solvent solution will harden as the solvent evaporates, leaving a clear, solid scintillator.

Films of the material can be easily manufactured. The epoxy or plastic can be coated onto a flat surface or a cylindrical lightpipe. Since the films are optically clear, the down-converted photons can reach a PMT placed some distance away.

Chapter 2

Preparation for the Study

2.1 Selecting matrices

We chose matrices based on the following criteria: good optical clarity and absence of any elements that may activate when exposed to neutrons. Activation is an issue in the design of many neutron detectors since activated elements are likely to give false counts and perhaps negatively impact on the performance of an experiment.

Plastics and epoxies, being organic compounds (C, H, O), have small activation levels. In this study, PMMA (polymethyl methacrylate), and polystyrene were used as plastic matrices (see Figure 2-1), and Stycast 1266 Clear Epoxy as a suitable epoxy matrix. All three matrices in their undoped form exhibit exceptional optical clarity.

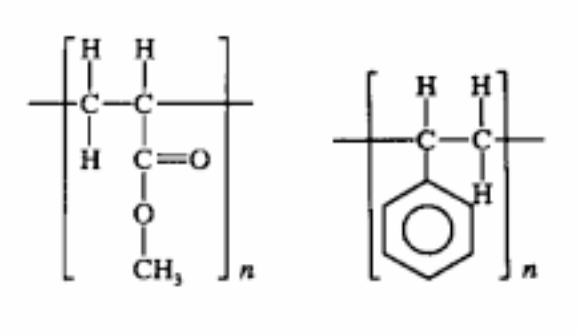

Figure 2-1: Polymethyl methacrylate (PMMA), left, and polystyrene, right. Figures from [3].

PROPERTY	^{10}B	^{6}Li
Thermal neutron capture cross section	3837 b	940.3 b
Reaction products	α, ^{7}Li	α, t
Total kinetic energy of ionizing particles	2.31 MeV (93.6%)	4.7 MeV

Table 2.1: Properties of boron-10 and lithium-6.

2.2 Selecting dopants

The dopants, alone or in combination, must perform two tasks: absorb the incoming thermal neutron and emit a signal that can be detected by available instruments. In our case, the signal we seek is a visible light scintillation that can be detected by conventional PMT's.

Boron-10 and lithium-6 are good candidates for neutron converters since they both have high thermal neutron capture cross sections, and upon neutron capture decay emitting energetic ionizing particles (alpha particles and nuclei) that should produce scintillations [4] [5] [6]. Their properties are summarized in Table 2.1.

When a boron-10 atom captures a thermal neutron, one of the following reactions occurs:

$$^{10}\mathrm{B} + n \longrightarrow \alpha + {}^{7}\mathrm{Li} + \gamma \qquad 93.6\%$$

$$^{10}\mathrm{B} + n \longrightarrow \alpha + {}^{7}\mathrm{Li} \qquad 6.4\%.$$

In the first reaction, the alpha particle carries 1.47 MeV, the lithium nucleus 0.84 MeV, and the gamma ray 0.48 MeV. In the second reaction, the alpha particle and the lithium nucleus carry all 2.79 MeV of available energy [4].

For lithium-6 atoms, the reaction is:

$$^{6}\mathrm{Li} + n \longrightarrow \alpha + {}^{3}\mathrm{H}.$$

The triton carries 2.7 MeV of kinetic energy, and the alpha particle 2 MeV [7]. The tritium nucleus is unstable; however, it has a halflife of 12.3 years, so we do not expect it to cause a significant number of false counts.

The alpha particles and ions transfer their energy to the surrounding matrix. Based on experiments (Section 5.6) conducted with only neutron converters (boric acid and lithium perchlorate) doped into epoxy matrices, we believe part of the energy of the alpha particles

and ions produces UV scintillations in the epoxy, similar to UV scintillations produced in liquid organic scintillators [8]. Since the plastic matrices are hydrocarbons of similar atomic composition and density, we believe the alpha particles and ions produce some amount of UV scintillation in the plastics as well.

These UV scintillations must be downconverted into the optical range, where our PMT's are most sensitive. Two such compounds that absorb UV radiation and emit visible light are sodium salicylate and TPB (tetraphenyl butadiene) [9]. Doped into the matrix, these UV downconverters flouresce when they absorb UV radiation.

In choosing suitable neutron converting compounds and UV downconverters, the most important requirement is that they be optically clear in the matrix, since opacity can lead to loss of downconverted photons, *i.e.*, loss of signal.

Chapter 3

Epoxy Film Development

3.1 Two-part Epoxies

Epoxies are thermosetting hydrocarbon resins. Two-part epoxies generally consist of: "Part A", a difunctional or higher epoxide (oxirane) molecule; and "Part B", (also called the catalyst or hardener) which can be a multifunctional amine or an acid anhydride. The two parts are mixed together and cured to form a hard, inert resin [10].

Our epoxy matrix is a standard two-part epoxy. The resin is a derivative of bisphenol glycidal ether. Part A is Stycast 1266 Clear Epoxy [11], and part B is any one of the following hardeners: Vestamin IPD [12], Vestamine TMD [13], Jeffamine D230 [14], or DuPont DCH99 [15]. The mixing ratio is approximate 3:1 by volume, part A to hardener.

We also added small amounts of benzyl alcohol during the mixing of the part A and hardener to help the hardener spread more evenly through the part A. Initial curing takes 8-16 hours at room temperature. During this time, the benzyl alcohol evaporates, leaving only the clear epoxy.

3.2 Dopants for the epoxy matrix

Since Stycast 1266 Clear Part A is a very viscous liquid, the dopants were dissolved into the hardener. We sought neutron converting compounds and UV downconverters that were soluble and optically clear in the hardener.

To test the solubilities, we added the solute to the hardener at a concentration of 2% solute by weight in the hardener. The solution was stirred in a magnetic stirrer for 20 hours.

COMPOUND	Sty B	Vest IPD	Vest TMD	Jeff D230	DCH99
Elemental boron (powder)	X				
Boron nitride	opaque	X			
Boric acid 97% ^{10}B	X	O	X	O	
Boron oxide		opaque			
Boron triiodide		X			
Lithium hexafluoroantimonate	X				
Lithium iodide	X	X			
Lithium sulfate		O			
Lithium nitrate		X			
Lithium perchlorate		O			
Lithium bromide		opaque			
Lithium chloride		opaque			
Lithium hydroxide		X	X		X
Lithium 2-ethylhexanoate				X	
Lithium 2,4-pentanedionate				opaque	
TPB		X	X	X	X
Sodium salicylate		O	O		

Table 3.1: Solubilities of neutron converters and UV downconverters in epoxy hardeners. **Sty B**: Stycast 1266 Clear Part B, **Vest IPD**: Vestamin IPD, **Vest TMD**: Vestamin TMD, **Jeff D230**: Jeffamine D230, **DCH99**: DuPont DCH99. **Opaque**: solution is opaque, **X**: solute does not dissolve, **O**: solution is clear and colorless. The solutions were stirred in a magnetic stirrer for 20 hours, at concentrations of 2% by weight in the hardener.

The solubilities and clarities of the tested compounds in various hardeners are summarized in Table 3.1. During the course of the study, we found that Vestamin IPD dissolved the widest variety of compounds.

Two neutron converters that were clear in the hardener were boric acid (H_3BO_3) and lithium perchlorate ($LiClO_4$) in Vestamin IPD. The final epoxy films prepared from the doped hardeners were clear as well.

TPB has a higher quantum efficiency than sodium salicylate [9]. However, we chose sodium salicylate as a UV downconverter for the epoxy films because TPB was insoluble in all the epoxy hardeners.

To test a wider variety of neutron converters and UV downconverters, we performed additional experiments where we dissolved the compounds into a variety of intermediate solvents (See Table 4.1), such as toluene and chloroform, and loaded the solutions into either epoxy part A's or the hardeners. We found that all the epoxies prepared this way were initially clear, but became opaque in 24 hours as the intermediate solvents evaporated.

3.3 Preparation of the doped epoxy films

After the compounds were completely dissolved in the hardener, the hardener solution was mixed with the Stycast 1266 Clear Part A. The epoxy solution was then placed in a dessicator attached to a pump. Pumping on the epoxy for approximately 30 minutes removed air bubbles that formed during the mixing. The result was an optically clear, bubble-free epoxy that could be coated onto acrylic rods.

Pumping on the epoxy did not appear to remove much of the neutron converters or the UV downconverter. (The compounds also have no vapor pressure.) The presence of the UV downconverter was verified by shining a UV lamp on the epoxy and observing fluorescence. The presence of neutron absorbing compounds was verified by placing the epoxy in a thermal neutron beam and using a BF_3 counter to measure the neutron flux density in front of and behind the epoxy. We believe that at most 20% of each dopant was lost during pumping.

We found that the addition of benzyl alcohol during the mixing process not only helped to spread the hardener out through the Part A, but also lowered the viscosity, making the air bubbles in the epoxy easier to pump out.

Chapter 4

Plastic Film Development

4.1 Plastic matrices

PMMA and polystyrene were chosen as suitable plastic matrices because of their exceptional optical clarity [16] and ease of handling. These plastics were obtained in powder and pellet form, and dissolved into various solvents such as toluene and THF (tetrahydrofuran). The solvents evaporated overnight, leaving a clear PMMA or polystyrene film.

For the plastic-based films, we sought a solvent that would simultaneously dissolve the matrix, neutron converter, and UV downconverter.

4.2 Dopants for the plastic matrices

The same neutron converting compounds as in the epoxy film development stage were tested. Solutes were added to the solvents at initial concentrations of 2% solute by weight in the solvent, then left to stir for 20 hours in a magnetic stirrer. The solubilities and clarities of the tested compounds in various solvents are summarized in Table 4.1.

COMPOUND	Tol	Eth	ChlB	Chlr	THF
Elemental boron (powder)	opq	X	opq		X
Boron nitride				opq	
Boric acid 97% ^{10}B	X		X	X	X
Boron oxide					X
Boron triiodide	red		red		
Lithium hexafluoroantimonate	X	O	X	X	O
Lithium iodide	X		opq		X
Lithium sulfate					X
Lithium fluoride	X		X	X	X
Lithium nitrate					O
Lithium perchlorate	X	O	X		O
Lithium bromide	X				
Lithium chloride	X				
Lithium hydroxide	X				
Lithium 2-ethylhexanoate	X		opq	O	X
Lithium cyclopentadienide	X				opq
Lithium 2,4-pentanedionate	X		X	X	X
TPB	O	O	O	O	O
Sodium salicylate		O			
PMMA	O	X	O	O	X
Polystyrene	O	O			O

Table 4.1: Solubilities of neutron converters, UV downconverters, and plastics in various organic solvents. **Tol**: toluene, **Eth**: ethyl ether, **ChlB**: chlorobenzene, **Chlr**: chloroform, **THF**: tetrahydrofuran. **Opq**: solution is opaque, **X**: solute does not dissolve, **O**: solution is clear and colorless, **red**: solution is transparent but reddish. The solutions were stirred in a magnetic stirrer for 20 hours, at concentrations of 2% solute by weight in the solvent.

4.3 Preparation of the doped plastic films

The following four plastic films seemed promising, since the solutions containing the plastic, neutron converter, and UV downconverter were all clear and colorless.

1) Lithium 2-ethylhexanoate ($LiOOC(C_2H_5)CHC_4H_9$), TPB, and PMMA in chloroform.

2) Lithium hexafluoroantimonate ($LiSbF_6$), TPB, and polystyrene in THF.

3) Lithium perchlorate ($LiClO_4$), TPB, and polystyrene in THF.

4) Lithium nitrate ($LiNO_3$), TPB, and polystyrene in THF.

Solutions were prepared with concentrations of 5% neutron converter by weight in the plastic, and 5% TPB by weight in the plastic. The dopant-matrix-solvent solution was then poured onto glass slides and left overnight at room temperature in a fume hood to allow the solvent to evaporate.

All four films were opaque once the solvent had dissolved. It was possible to prepare clear, colorless films doped with only the UV downconverter; we therefore attribute the opacity of the films to the presence of the neutron converting compound.

To examine the clarities of a wider variety of neutron converters in plastic, we tried two additional methods. We slowly mixed UV downconverter-doped solvents with neutron converter-doped solvents — the "mixing solvents" method commonly employed in chemistry. A second technique consisting of adding the chemical additive TMEDA (tetramethylethylenediamine) to the solvents to allow them to dissolve a wider variety of compounds. Both methods yielded doped plastic films that were opaque once the solvents evaporated.

We did not prepare any doped plastic films for neutron irradiation since none of the films were clear.

Chapter 5

Epoxy Films: Neutron Irradiation Tests

5.1 Preparation of the rods

Because of their exceptional optical clarity, acrylic rods (5/8" diameter) were selected as lightpipes to couple the epoxy film to the PMT. Acrylic has the additional advantage that it does not activate when exposed to neutrons, unlike glass which contains silicon. We cut the rods into 12.5" segments, and polished the ends with plastic polish to reduce the amount of scattering at the ends.

The doped epoxy (after the bubbles were pumped out) was coated onto one end of the polished acrylic rods. The epoxy film covered about 3" of the length of the rod. The rods were kept at room temperature and held vertical for 24 hours to cure.

We prepared four different rods:

1) Rod Bo: 1.4% Boric Acid (97% B-10) by weight (b.w.) in the final epoxy.
1.5% Sodium salicylate b.w. in the final epoxy.
Benzyl alcohol added during mixing.
Pumped on epoxy to remove bubbles.
Average Film thickness: 0.09 mm.
Even coating.
Optical clarity: clear, no bubbles.

2) Rod Bo-b: 1.4% Boric Acid (97% B-10) b.w. in the final epoxy.
1.5% Sodium salicylate b.w. in the final epoxy.
No benzyl alcohol added during mixing.
Pumped on epoxy to remove bubbles.
Even coating.
Optical clarity: clear, some bubbles

3) Rod Bo-bp: 1.4% Boric Acid (97% B-10) b.w. in the final epoxy.
1.5% Sodium salicylate b.w. in the final epoxy.
No benzyl alcohol added during mixing.
No pumping on epoxy to remove bubbles.
Uneven coating.
Optical clarity: clear, many bubbles.

4) Rod Li: 1.4% Lithium perchlorate b.w. in the final epoxy.
1.5% Sodium salicylate b.w. in the final epoxy.
Benzyl alcohol added during mixing.
Pumped on epoxy to remove bubbles.
Uneven coating.
Optical clarity: clear, no bubbles.

The rods were then wrapped in a sheet of aluminum foil and wound with Mylar tape to make them light tight. The epoxy-covered tip of the rod was capped with electrical tape to seal any light leaks. The other tip was left open for coupling to the PMT photocathode.

5.2 Irradiation setup

The experiments were conducted at the Massachusetts Institute of Technology's Nuclear Reactor Laboratory (NRL). NRL has a number of thermal neutron beamports; we used beamport 4DH4.

The 4DH4 port has a diffraction crystal whose orientation can be adjusted using an external knob. The advantage of this setup is twofold: we obtain a highly monoenergetic thermal neutron beam, and we also do not "look" directly into the reactor core, eliminating virtually all of the gamma flux. Our setup is shown in Figure 5-1.

Using a calibrated BF_3 counter, we determined the flux density to be 6600 ± 780 thermal neutrons per second per cm^2. The beam has a circular cross section, approximately 3.8 cm in diameter.

Optical grease was applied to the uncoated end of the rods and attached to the face of the PMT. All the joints were wrapped in electrical tape to make them light tight.

We used a 2" bialkali, 12 stage Burle C31000M photomultiplier tube [17] in a Products for Research [18] cooling chamber to minimize the dark counts. The temperature of the cooler was kept at 243 K. The PMT was biased at –1600 V for all measurements.

Signals were analyzed using a Canberra Series 35 multichannel analyzer using its built-in pre-amplifier. For all measurements, real time was approximately 301 s with a dead time of 0.7%. Amplifier gain, ADC gain, and lower level discriminator (LLD) settings were kept constant for all the measurements.

5.3 Irradiation procedure

Each rod was tested in three configurations.

1) *Beam open, no blocks.* This setup corresponded to the thermal neutron beam on, the epoxy-coated end of the rod in the beam, and no blocks between the rod and the beamport. For this and all other configurations, the thermal neutron beam only illuminated the coating of epoxy on the sides of the rod, and not the coating at the tip.

2) *Beam open, boron block.* This setup is identical to "Beam on, no blocks" except a 2" thick brick of boron was placed between the rod and the beamport. Using the calibrated BF_3 counter, we verified that close to all neutrons from the port were being absorbed by the brick.

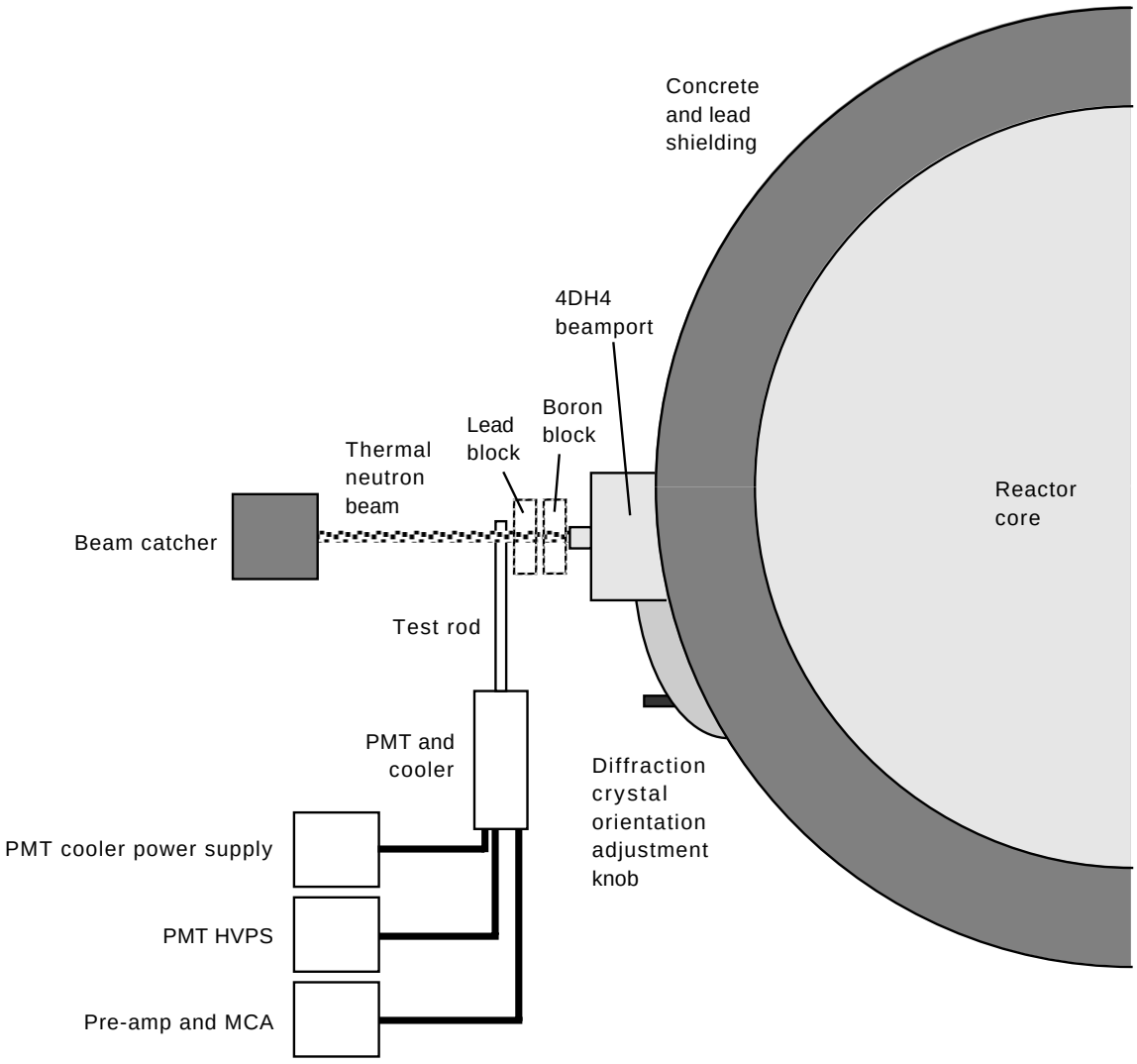

Figure 5-1: Experimental setup at the MIT reactor.

3) *Beam open, boron and lead block.* In addition to the boron block, a 2" thick brick of lead was placed between the rod and the boron block to block any gammas coming from the beamport or the irradiated boron block.

The positions of the rod and the PMT were not altered for the above configurations.

5.4 Irradiation results

We present the results of the four epoxy-coated rods: Bo, Bo-b, Bo-bp, and Li. The graphs are pulse height histograms — channel 900 (horizontal axis) corresponds to 250 mV, with each channel having a bin "width" of 0.28 mV. (The magnitudes of these voltages are of pulses at the anode of the PMT, *i.e.*, before they are amplified by the MCA and pre-amp.) Each "count" (vertical axis) is a burst of photons from the UV downconverter after a single neutron capture event. For all the pulse height histograms, data were collected for 300 s (live time).

Figures 5-2, 5-3, 5-4, and 5-5 show the number of counts obtained with each rod in the three different configurations.

Figures 5-6, 5-7, 5-8, and 5-9 show scans where the "Boron and lead block" scan has been subtracted from the "No blocks" scan. This gives a plot of the scintillations due only to neutron captures. We call "neutron capture" scans those scans where the "Both blocks" scan has been subtracted from the "No blocks" scan.

Figures 5-10, 5-11, 5-12, and 5-13 are scans where the "Boron and lead block" scan has been subtracted from the "Boron block" scan. Since the 4DH4 beamport does not look directly into the reactor core, we expect no significant difference between these two scans. Differences between these scans will alert us to sources of systematic or random error; we refer to these scans as "error" scans.

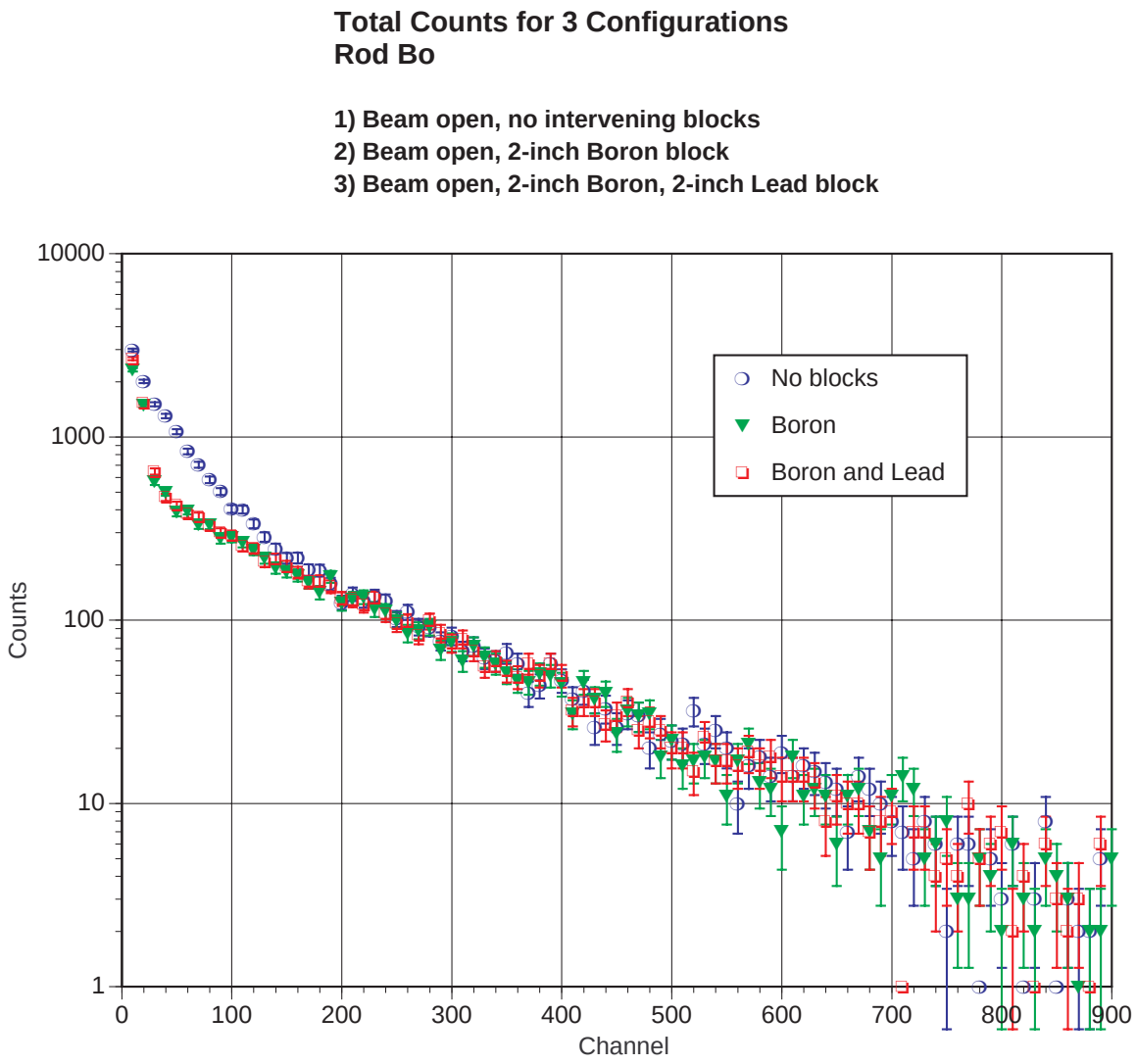

Figure 5-2: Boron Rod Bo. Counts for three configurations. Error bars are for 1 standard deviation.

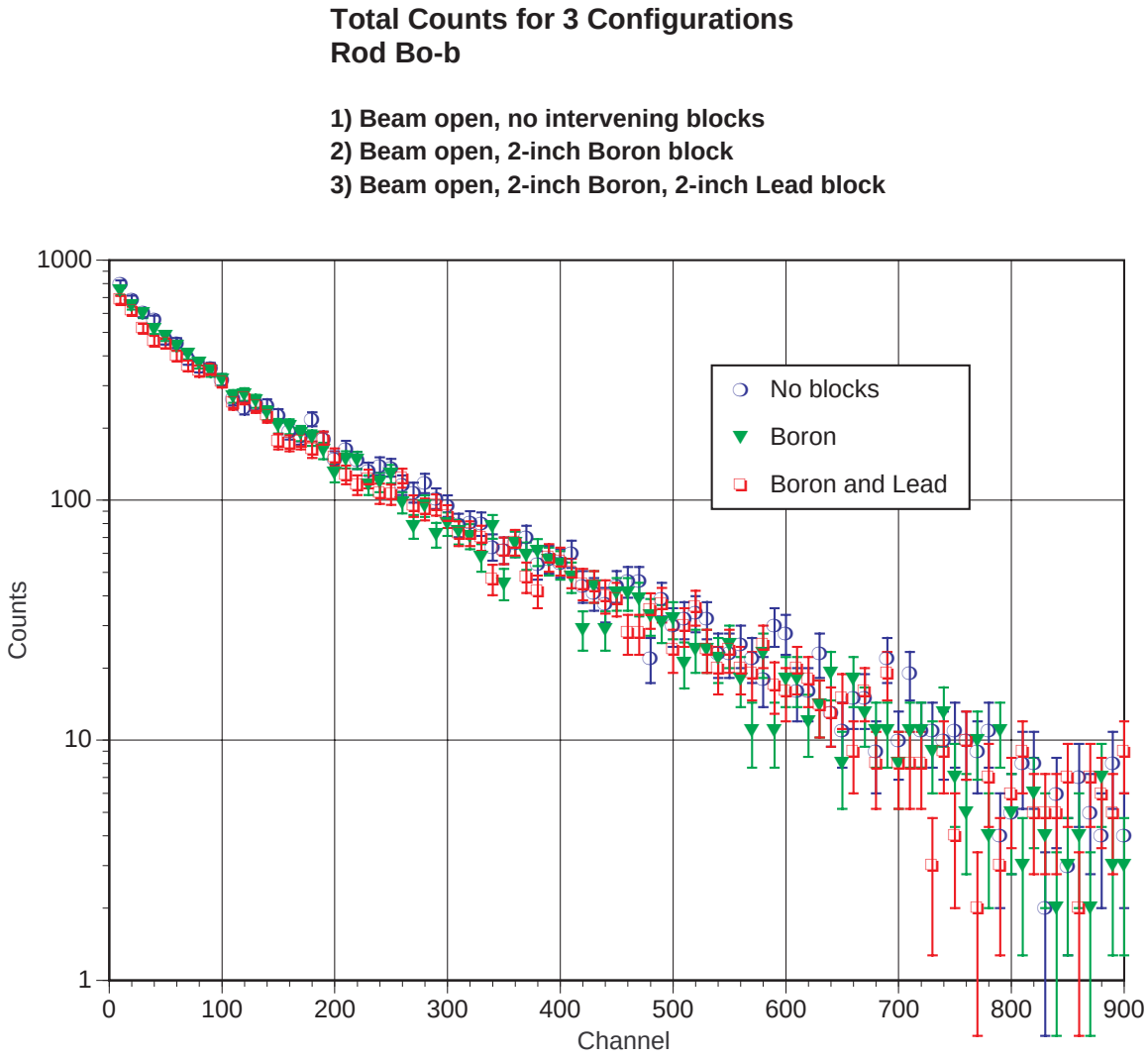

Figure 5-3: Boron Rod Bo-b. Counts for three configurations. Error bars are for 1 standard deviation.

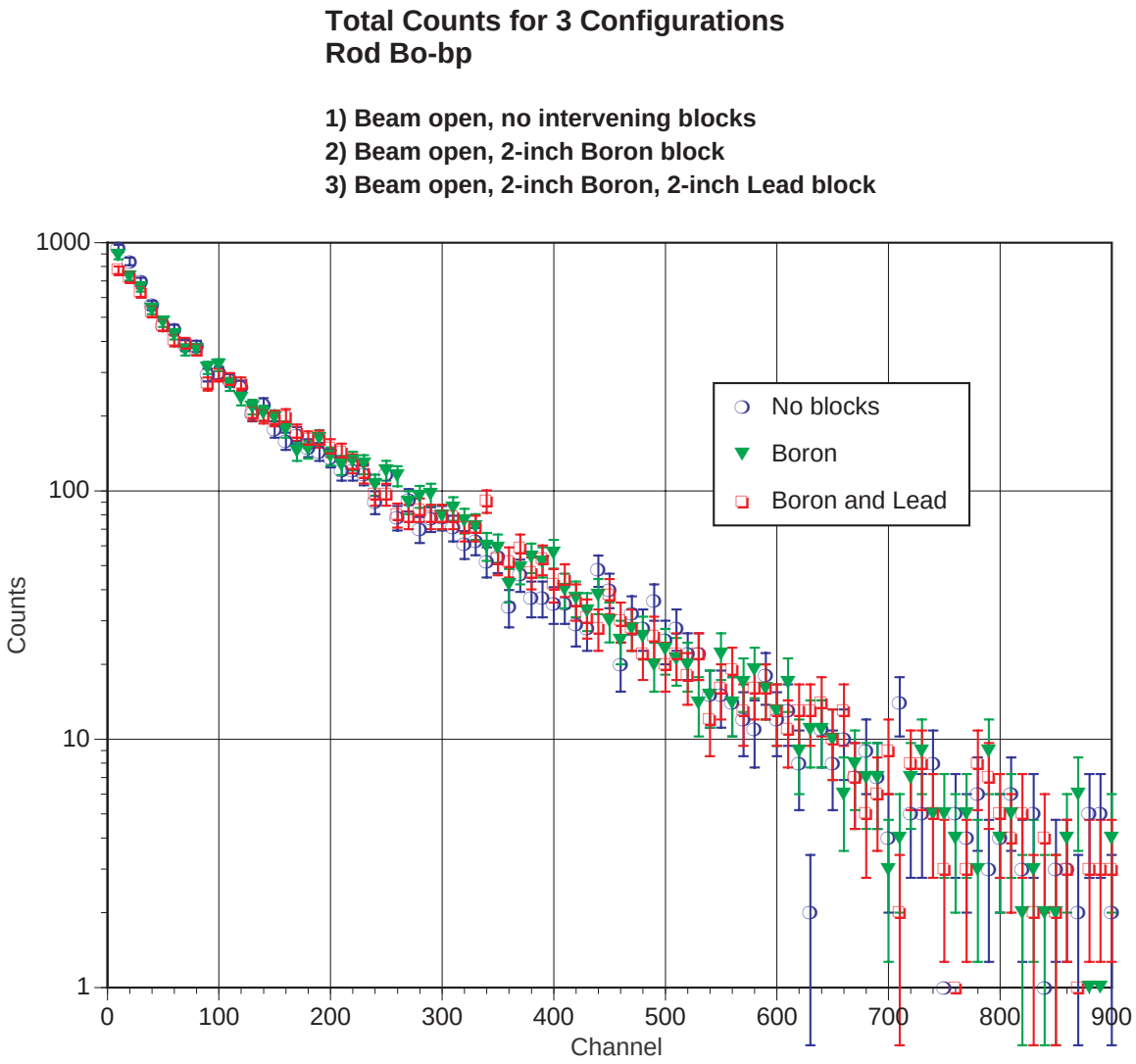

Figure 5-4: Boron Rod Bo-bp. Counts for three configurations. Error bars are for 1 standard deviation.

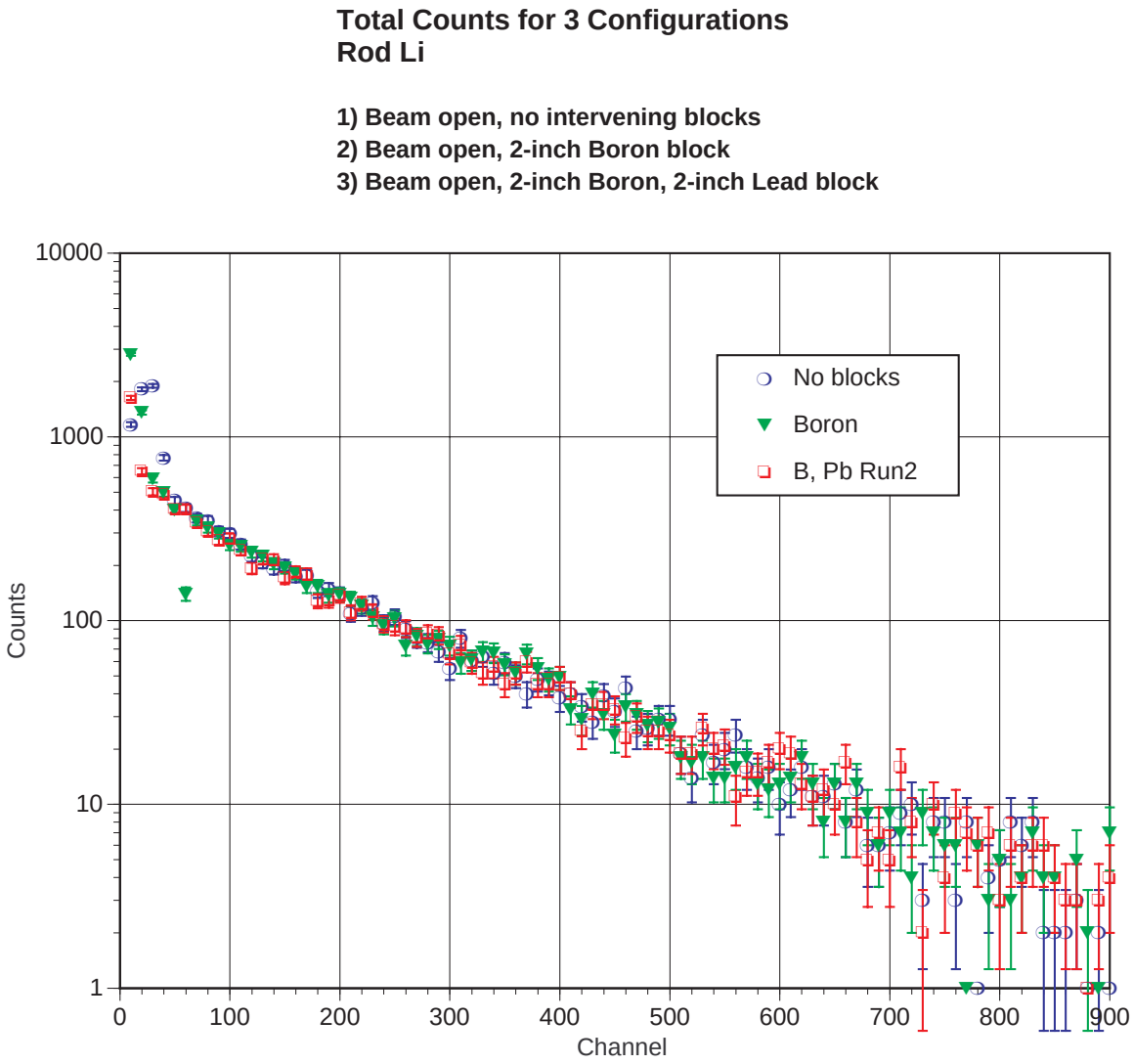

Figure 5-5: Lithium Rod Li. Counts for three configurations. Error bars are for 1 standard deviation.

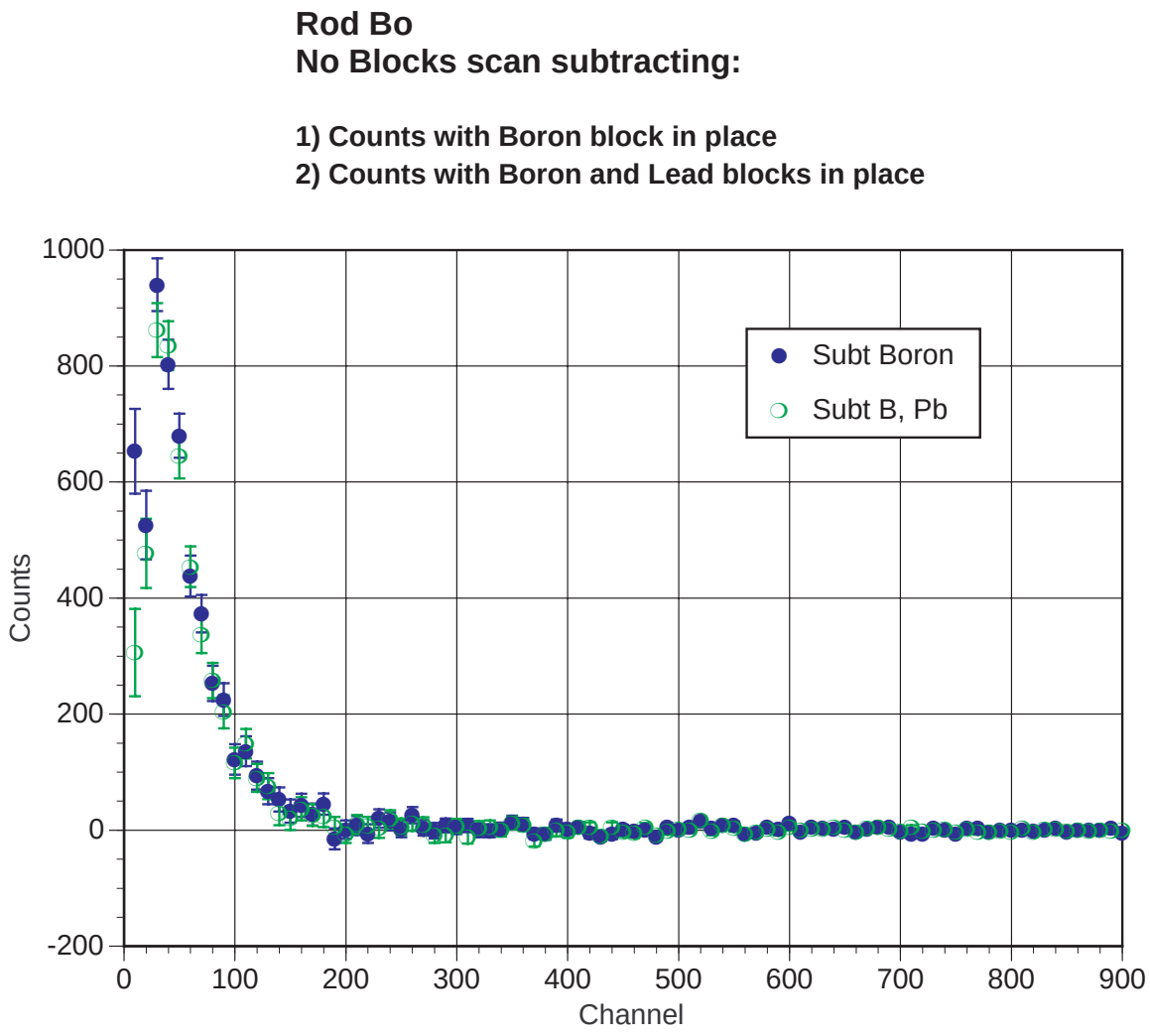

Figure 5-6: Boron Rod Bo. "Background" subtracted by subtracting the scans with both intervening blocks from the scan with no intervening blocks.

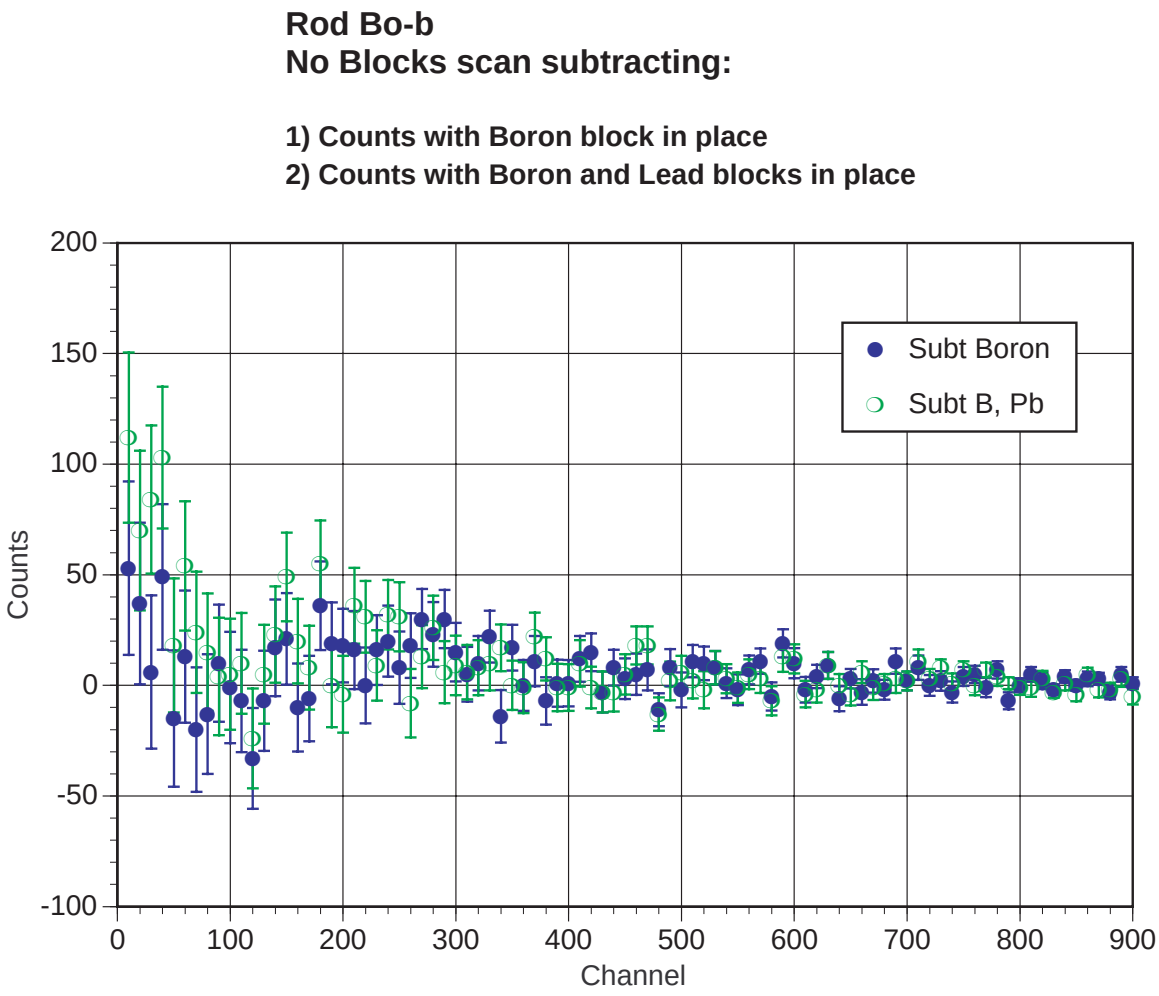

Figure 5-7: Boron Rod Bo-b. "Background" subtracted by subtracting the scans with both intervening blocks from the scan with no intervening blocks.

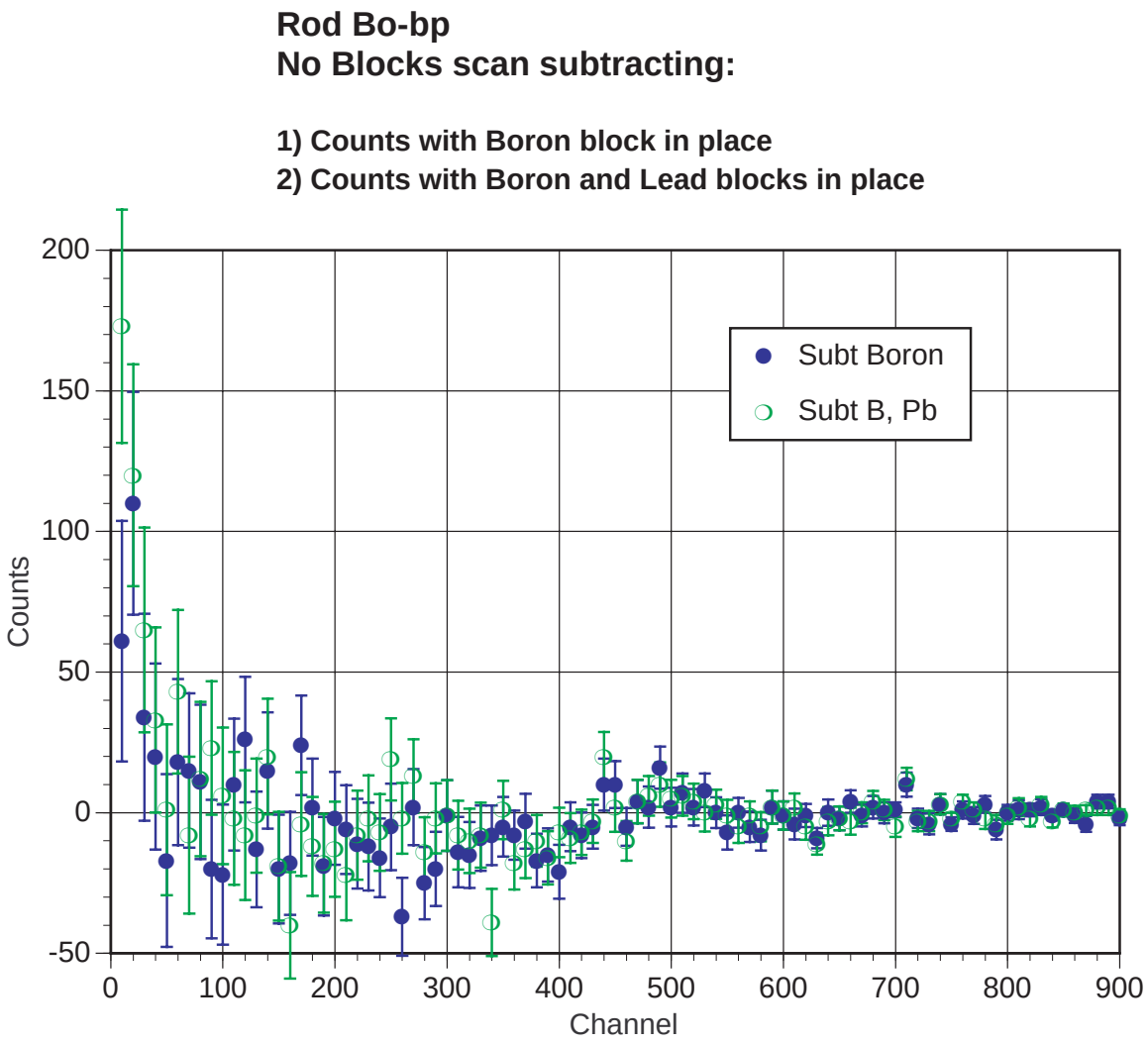

Figure 5-8: Boron Rod Bo-bp. "Background" subtracted by subtracting the scans with both intervening blocks from the scan with no intervening blocks.

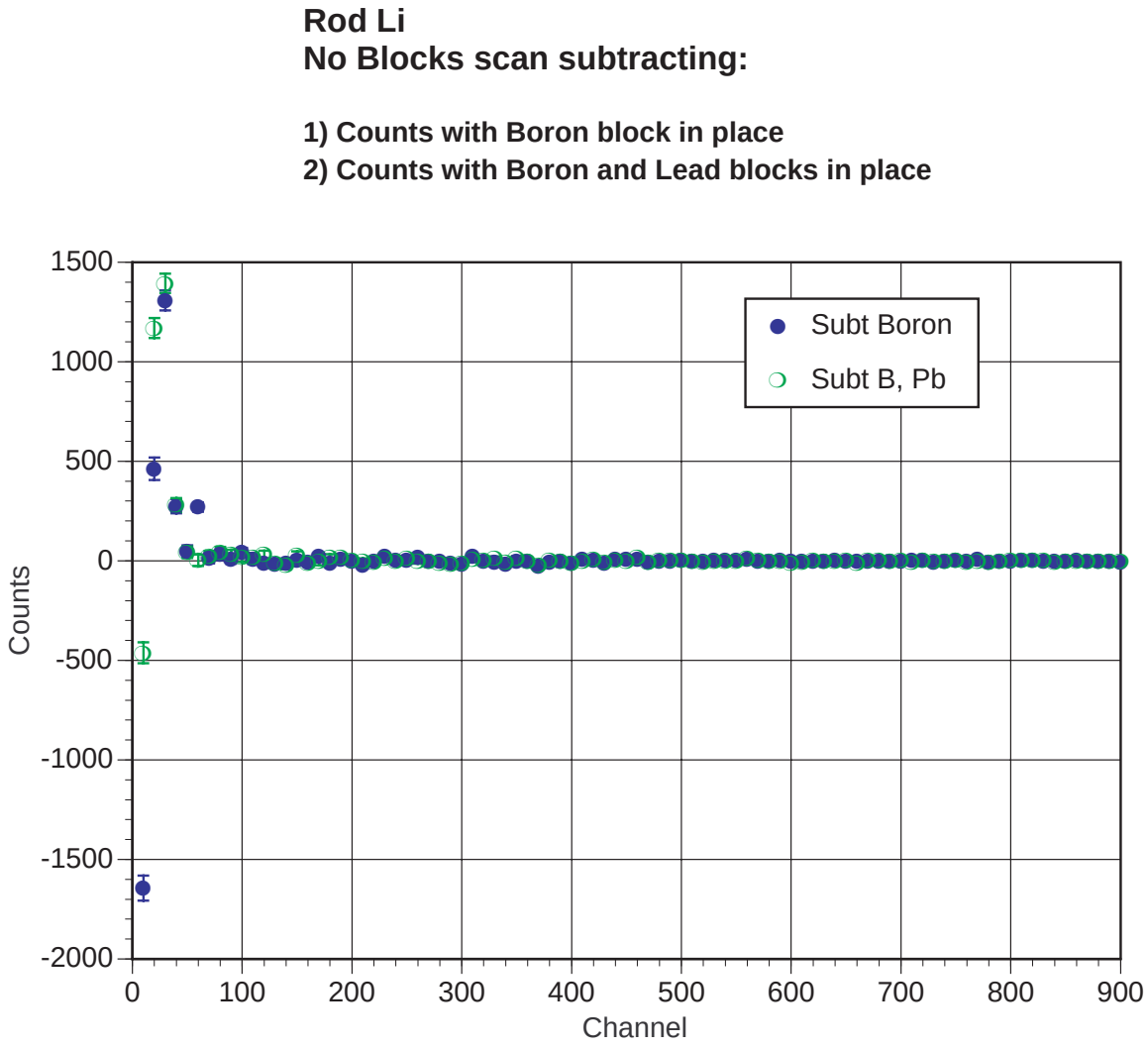

Figure 5-9: Lithium Rod Li. "Background" subtracted by subtracting the scans with both intervening blocks from the scan with no intervening blocks.

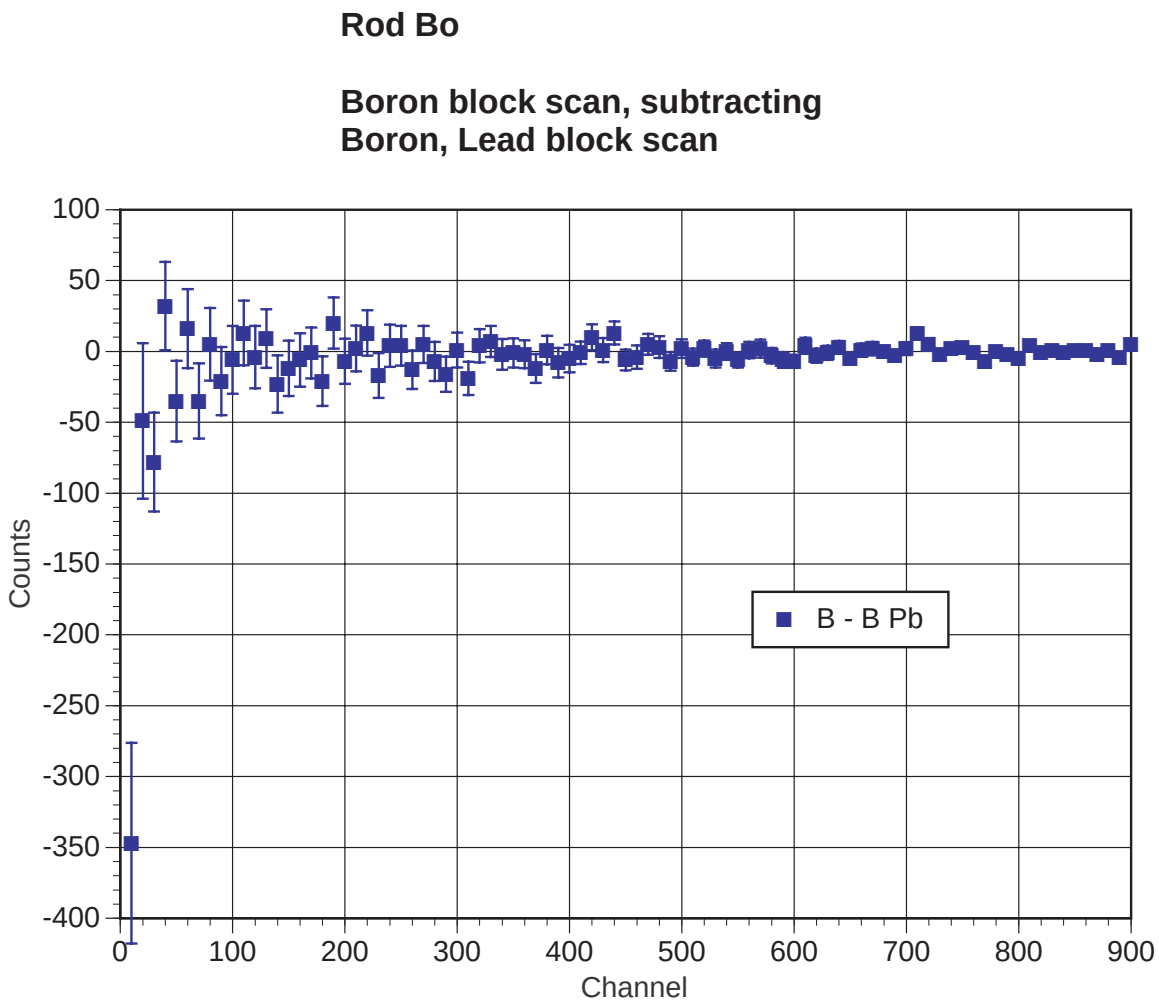

Figure 5-10: Boron Rod Bo. "Boron and lead blocks" scan subtracted from the "Boron block" scan. We expect to find no difference between these two scans.

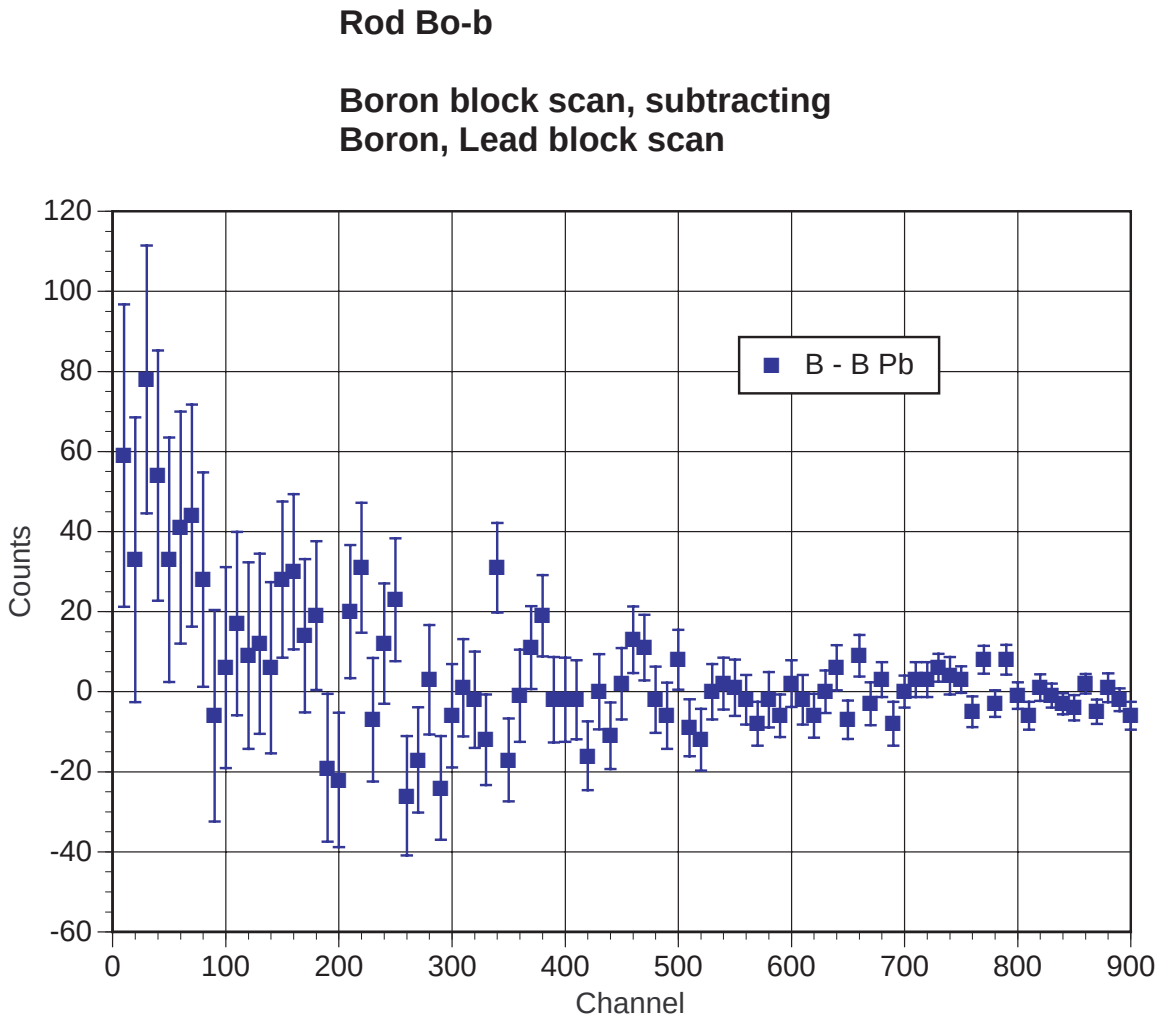

Figure 5-11: Boron Rod Bo-b. "Boron and lead blocks" scan subtracted from the "Boron block" scan. We expect to find no difference between these two scans.

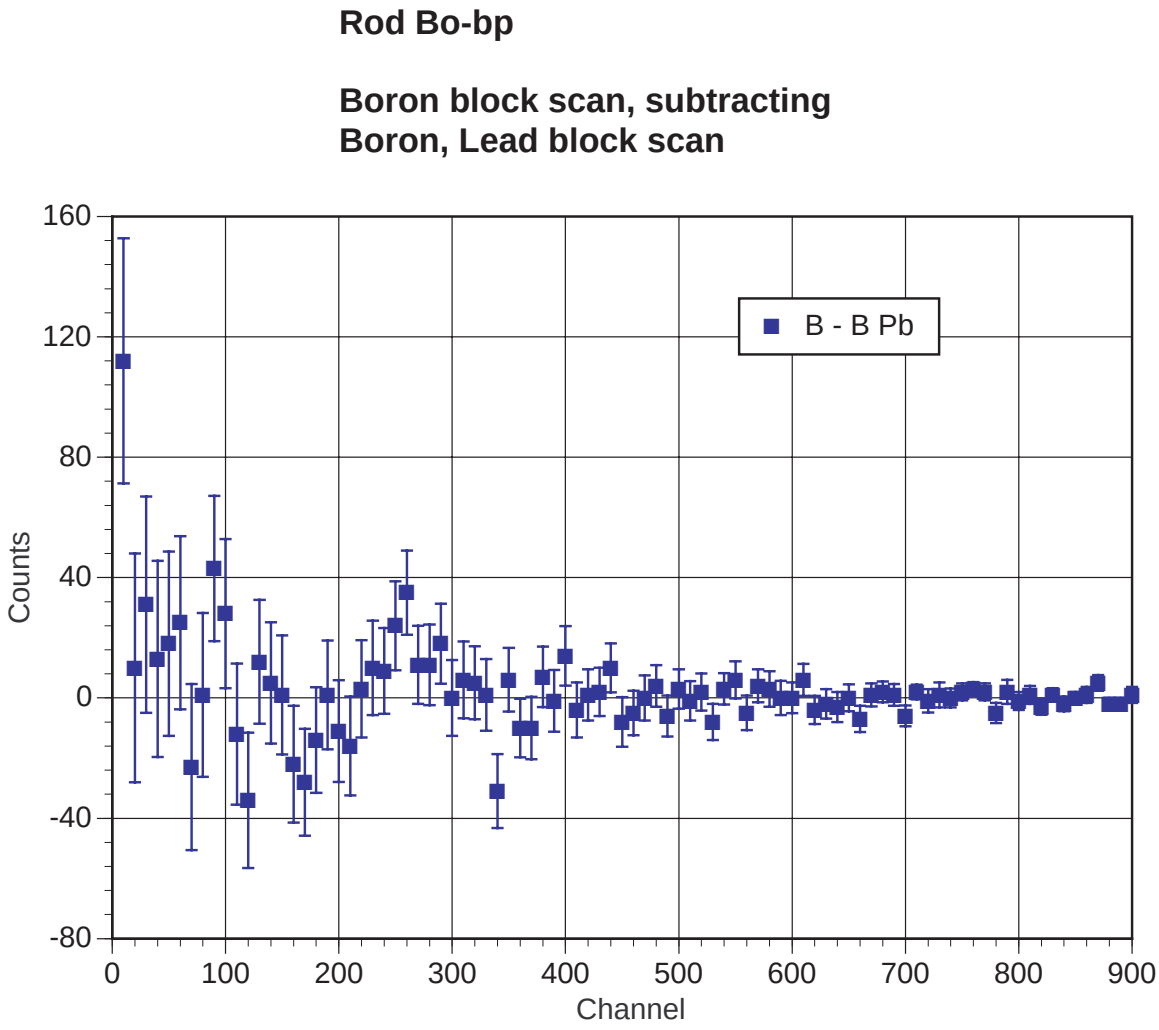

Figure 5-12: Boron Rod Bo-bp. "Boron and lead blocks" scan subtracted from the "Boron block" scan. We expect to find no difference between these two scans.

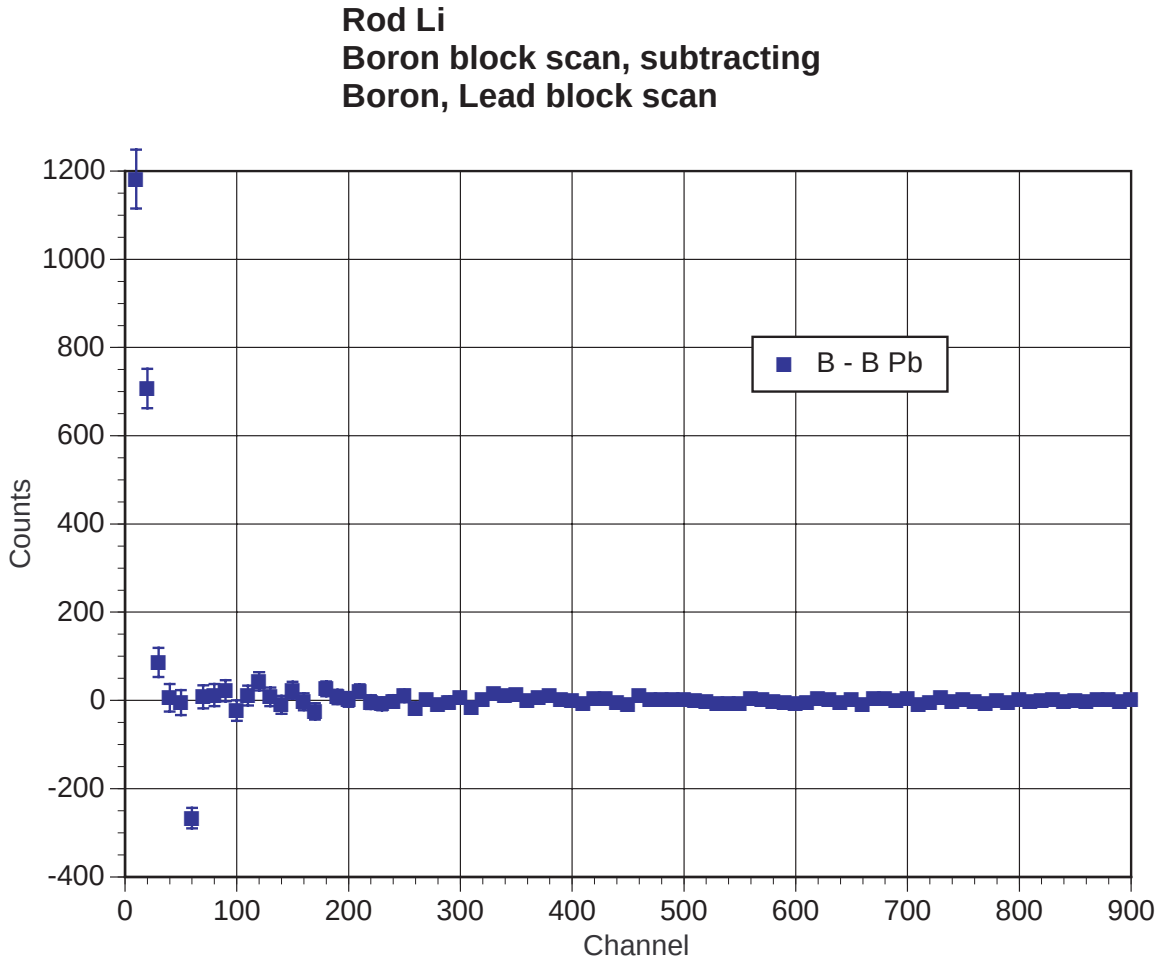

Figure 5-13: Lithium Rod Li. "Boron and lead blocks" scan subtracted from the "Boron block" scan. We expect to find no difference between these two scans.

We observed evidence for neutron capture events with Rod Bo (Figure 5-6), but not for the three other rods (Figures 5-7, 5-8, and 5-9). We believe this is due to poor transmission of the downconverted light in rods Bo-b, Bo-bp, and Li. Rod Li's setup also appeared to suffer from drifts in the electronics, as evidenced by the error scan (Figure 5-13).

The light transmission tests are discussed in the following section. The full discussion of the data is presented in Section 6.2.

5.5 Light transmission tests

Tests were conducted to determine the light transmission of our lightpipes.

We placed each rod in a light tight cardboard tube with one end attached to a PMT. The other tip was illuminated by a blue LED held 1 cm away from the tip. We used the same Burle C31000M PMT, biased at –1600 V. The results of the experiments are given in Figure 5-14. For comparison, we conducted additional tests with an acrylic rod with no epoxy coating, and one test with no intervening lightpipe (not shown).

We found that Rod Bo was the best lightpipe in the tip illumination test, transmitting light nearly as efficiently as the uncoated acrylic rod. At an LED voltage of 2.446 V, the other rods' transmission as percentages of that of Rod Bo were: Rod Bo-b 60%, Rod Li 57%, and Rod Bo-bp 33%.

Rod Bo had the most uniform and bubble-free epoxy coating. Rod Bo-b had a uniform coating save for a few bubbles (0.5 to 1 bubble per cm^2). Rod Li had a coating of epoxy that was free of bubbles but suffered from variations in film thickness along the length of the rod. The variations in thickness were up to 10 times the thickness of the thinnest part of the coating. Rod Bo-bp had a bubble-ridden epoxy coating (at least 20 bubbles per cm^2). Additional tests where we illuminated the rods from the side using a flashlight bulb showed that such irregularities were significant scattering centers. From these tests we concluded that the presence of bubbles in the film and variations in coating thickness reduce the lightpipes' light transmission.

To obtain values for the absolute light transmission of the rods, we performed a tip illumination test with geometries identical to the setup decribed above, except for the lack of any lightpipes. With this setup, the PMT "saw" a solid angle of $8\pi \cdot 10^{-4}$ sr. We used this data to compute the expected PMT voltage had we captured LED light over $5.2\pi \cdot 10^{-1}$ sr.

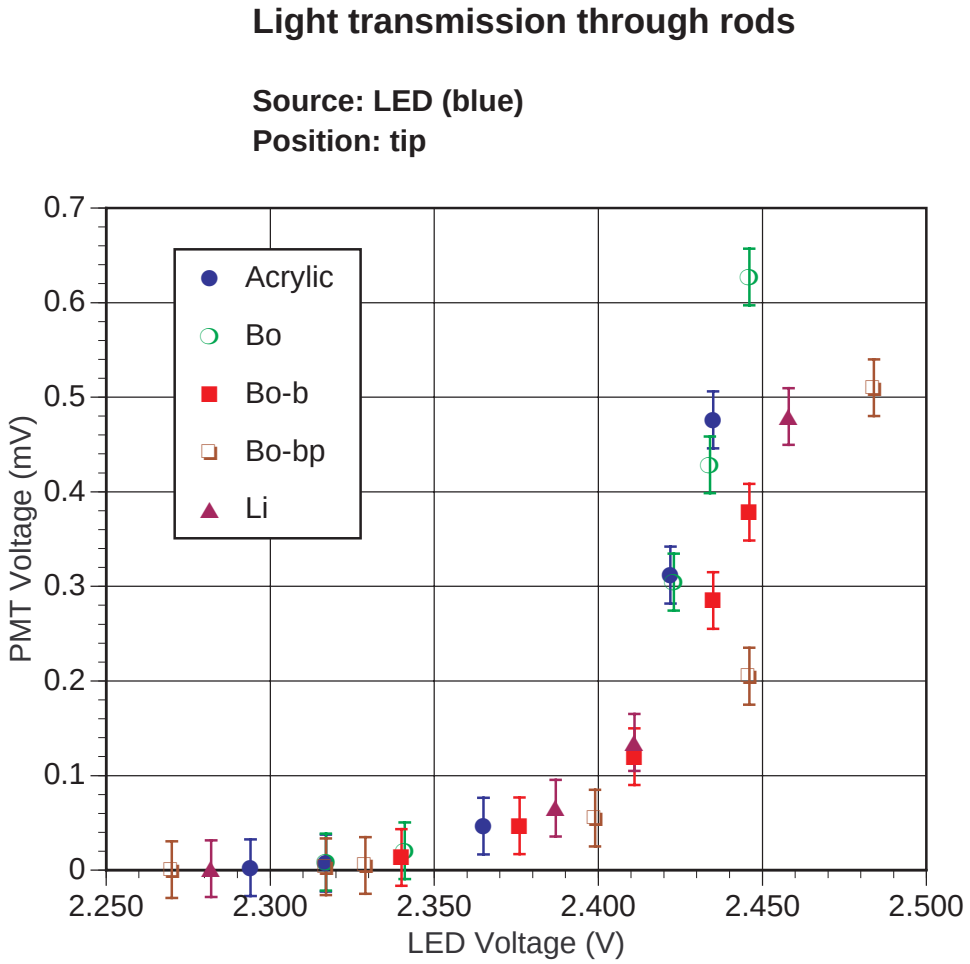

Figure 5-14: Light transmission through the rods. The source is a blue LED at the tip of the rods.

The assumption we make in this computation is that the LED's light intensity is roughly constant over $5.2\pi \cdot 10^{-1}$ sr, looking straight into the "axial" direction of the LED. This light is very directional, but the assumption is not a bad one since we are looking only at the frontal, narrow cone.

Acrylic has a refractive index of approximately 1.49. For a light source placed at one end of a 5/8" diameter rod, a cone of light corresponding to $5.2\pi \cdot 10^{-1}$ sr will undergo total internal reflection and be piped down to the other end. Comparing the predicted PMT response to a $5.2\pi \cdot 10^{-1}$ sr light cone at a set LED voltage to the response with the lightpipe in place gives us a measure of the absolute light transmission of each rod.

The uncoated acrylic rod's light transmission was approximately 1.5%, and Rod Bo's 0.9%. The low values are believed to be caused by scratches, heavy fingerprints, and other scattering centers on the sides of the lightpipe.

5.6 An earlier experiment: no UV downconverter

We conducted an earlier experiment during the epoxy film development stage to determine whether epoxy matrices doped only with neutron converters scintillate in the visible range when exposed to the heavy ionizing particles that result from neutron capture.

We prepared rods with epoxy films containing only the enriched boric acid (concentrations of 2.5%, 1.3%, 0.13%, and 0.01% boric acid b.w. in the epoxy). A similar set of lithium films was also prepared using lithium perchlorate (1.3% b.w. in the epoxy). Small amounts of benzyl alcohol were added to all the epoxies during mixing, and air bubbles were pumped out to make a clear film. These rods were identical to the final test rods in composition and preparation, except for the absence of the UV downconverter.

The rods were irradiated in configurations similar to the setup mentioned earlier. The rods were coupled to a 1/2" RCA 87-52 PMT kept at room temperature, and irradiated with thermal neutrons from NRL's 4DH3 beamport. 4DH3 has a reported average thermal neutron flux density of $7.4 \cdot 10^8$ neutrons per second per cm^2 [19]. "Turning off" the neutron beam was achieved by closing a mechanical shutter.

We observed no difference between the "beam on" and "beam off" scans, both for the lithium and the boron rods. We concluded that the heavy ions produced by the neutron capture do not cause visible light scintillations in the epoxy.

Successful experiments with a UV downconverter present in the epoxy suggested that part of the energy of the alpha and other ionizing particles go to UV scintillations in the epoxy.

Chapter 6

Discussion and Conclusions

6.1 Theoretical expectations for the epoxy films

The expected neutron capture probabilities for a doped film are given by the following expression:

$$P = n\sigma L,$$

where P is the probability that a capture event occurs, n is the density of the boron or lithium atoms in atoms per cm^3, σ is the thermal neutron capture cross section of boron or lithium in barns, and L is the average thickness of the film in cm.

When an area A of the film is exposed to a neutron flux density of ϕ for a time t, we expect to detect N neutrons:

$$N = (n\sigma L)\phi A t \kappa,$$

where κ is a unitless light transmission parameter; its value corresponds to the fraction of neutron capture events that are successful in generating a light pulse that is detected by the PMT. κ is a function of several efficiencies: UV to visible downconversion, transmission through the epoxy, transmission through the acrylic lightpipe, and transmission to the photocathode. For now, we set $\kappa = 1$, *i.e.*, we assume that the PMT receives enough photons from each capture event to register a signal.

PARAMETER	VALUE
n (^{10}B atoms per cm^3)	$1.2 \cdot 10^{20} \pm 1.9 \cdot 10^{19}$
σ (barns)	3837
L (mm)	0.09 ± 0.01
ϕ (neutrons per second per cm^2)	6600 ± 780
A (cm^2)	5.96 ± 0.80
t (seconds)	301 ± 1
κ	1
N (neutrons)	$4.9 \cdot 10^4 \pm 1.3 \cdot 10^4$

Table 6.1: Parameters involved in the computation of expected neutron counts for the boron rod Bo.

6.2 Comparison with the experimental results

Figures 5-6, 5-7, 5-8, and 5-9 are "neutron capture" scans. Rod Bo showed good evidence of neutron capture; pulses due to capture events ranged from 6 mV to 33 mV, with a most probable pulse height of approximately 8.5 mV. An examination of the "error scan" for Rod Bo shows no anomalies except in the first few channels. We attribute this discrepancy to normal jitter in the electronics immediately around the voltage cutoff set by the lower level discriminator of the pre-amplifier.

A calculation of expected neutron capture events for Rod Bo is:

$$N_{Bo(Theory)} = 4.9 \cdot 10^4 \pm 1.3 \cdot 10^4.$$

The error is computed from parameters described in Table 6.1.

Computing the area under the neutron capture curve (boron and lead block subtracted) for Rod Bo gives us an observed N of:

$$N_{Bo(Experiment)} = 5.6 \cdot 10^4 \pm 0.2 \cdot 10^4.$$

The two values of N are plotted in Figure 6-1.

We found that the theory and measurements agree very well for Rod Bo. The observations suggest that just enough photons from each capture event reach the PMT to give a signal.

We observed no significant number of counts with Rods Bo-b and Bo-bp. (Figures 5-7

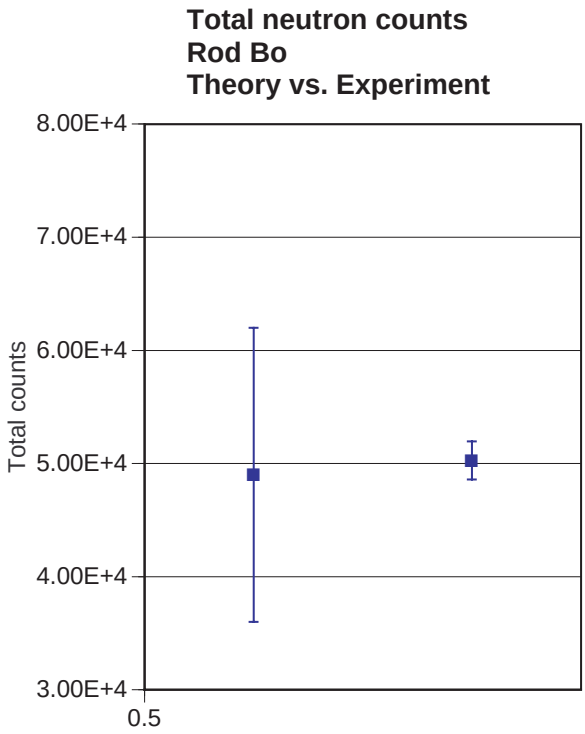

Figure 6-1: Total counts for Rod Bo. Calculated from theory (left) and observed (right).

and 5-8). We believe that this is due to the poor light transmission of the rods. Rod Bo-b has a transmission of 60% relative to Rod Bo. This would move the most probable pulse height of expected neutron events to about 5 mV. Similarly, Rod Bo-bp, with a light transmission of 33% relative to Rod Bo, would have a most probable pulse height of 2.8 mV. For both rods, there is some evidence of a tail of the neutron capture peak in the first few channels. Rod Bo-b shows a slightly wider portion of the tail, as expected from the respective light transmission values. The "error scans" (Figures 5-11 and 5-12) for both Rod Bo-b and Bo-bp show no significant anomalies.

Rod Li showed wide variations in the error scan (Figure 5-13). Since we expect no differences between the scan with only the boron block and the scan with both blocks, we suspect variations in the high voltage bias or drift in the electronics.

6.3 Ionizing particles' energy transfer to UV scintillations

From the pulse heights of neutron capture events in Rod Bo, we can compute a rough estimate of the fraction of the energy of the ionizing particles that produces UV scintillations in the epoxy.

The magnitude of the pulses we expect from the scintillations is given by:

$$V_{pulse}(volts) = f_{UV}\ f_{UVT}\ f_{vis}\ f_{visT}\ f_{QE} \cdot 50,$$

where f_{UV} is the fraction of the energy of the ionizing particles that produces the UV scintillations, and f_{UVT} is the fraction of the UV light that is transmitted by the epoxy film to the downconverter. f_{vis} is the quantum efficiency of the sodium salicylate, f_{visT} is the fraction of visible light transmitted through the epoxy-coated acrylic lightpipe, and f_{QE} is the quantum efficiency of the PMT.

A numerical factor of 50 is computed from the following parameters: current gain of the PMT ($1.6 \cdot 10^6$), solid angle of the piped light (0.5π sr), 4% loss at each optical surface (78% transmission for 6 surfaces), a presumed UV photon energy of 6 eV (corresponding to 200 nm), and a scintillation pulse duration of order 10 ns.

f_{vis} of sodium salicylate is approximately 0.37 [20], and f_{QE} is about 20% [17]. For Rod Bo, we measured f_{visT} to be 0.9%.

The most probable pulse height for Rod Bo was 8.5 mV. Assuming that the thin coating of epoxy does not absorb any UV photons ($f_{UVT} = 1$), we estimate that roughly 25% of the energy of the ionizing particles goes towards producing UV photons in the epoxy. Equivalently, our model and measurements agree to within a factor of four.

6.4 Future directions

Doped epoxy films show promise as a versatile detector for thermal and perhaps lower energy neutrons. The most obvious future improvement to our setup involves boosting the pulse heights of neutron capture events. We believe that polishing the sides of the lightpipes will increase the pulse height. Boosting the light transmission of the lightpipes to 25% will place our neutron capture peak pulse height at approximately 230 mV, at the far end of our pulse height histogram.

Bibliography

[1] W. D. Allen. *Neutron Detection*. Philosophical Library, Inc., 1960.

[2] J. M. Doyle, R. Golub, G. Greene, and S. Lamoreaux. Determination of the neutron lifetime using magnetically trapped neutrons, 1994. NSF grant proposal.

[3] I. I. Rubin, editor. *Handbook of plastic materials and technology*. John Wiley and Sons, Inc., 1990.

[4] L. M. Bollinger, G. E. Thomas, and R. J. Ginther. Neutron detection with glass scintillators. *Nuclear Instruments and Methods*, 17:99, 1962.

[5] K. H. Abel, R. J. Arthur, M. Bliss, D. W. Brite, R. L. Brodzinski, R. A. Craig, B. D. Geelhood, D. S. Goldman, J. W. Griffin, R. W. Perkins, P. L. Reeder, W. R. Richey, K. A. Stahl, D. S. Sunberg, R. A. Warner, M. J. Weber, and N. A. Wogman. Performance and applications of scintillating glass fiber neutron sensors. Pacific Northwest Laboratory., 1993.

[6] S. C. Curran. *Luminescence and the scintillation counter*. Academic Press Inc., 1953.

[7] P. Ottonello, G. A. Rottigni, G. Zanella, and R. Zannoni. Slow neutron imaging using scintillating glass optical fibers. *Nuclear Instruments and Methods in Physics Research A*, 349:527, 1994.

[8] W. D. Allen. *Neutron Detection*. Philosophical Library Inc., 1960.

[9] W. M. Burton and B. A. Powell. Fluorescence of tetraphenyl butadiene in the vacuum ultraviolet. *Applied Optics*, 12(1):87, 1973.

[10] G. S. Brady and H. R. Clauser. *Materials Handbook*. McGraw-Hill, Inc., 1991.

[11] Stycast 1266 Clear Epoxy, manufactured by Grace Specialty Polymers.

[12] Vestamin IPD, 3-Aminomethyl-3,5,5,-trimethylcyclohexylamine, manufactured by Hüls AG.

[13] Vestamin TMD, 2,2,4-Trimethyl hexamethylene diamine and 2,4,4-Trimethyl hexamethylene diamine, manufactured by Hüls AG.

[14] Jeffamine D230, polyoxypropylenediamine, manufactured by Huntsman.

[15] DCH99, 1,2-Diaminocyclohexane, manufactured by Du Pont Chemicals.

[16] J. B. Birks. *The theory and practice of scintillation counting.* Pergamon Press, 1964.

[17] *Burle photomultipliers product guide*, 1990.

[18] *Housings for PMT's and other low level detectors*, 1995.

[19] F. Lambert. Design and construction of the second version of the prompt gamma neutron activation analysis facility at the MIT nuclear reactor. MIT Nuclear Reactor Laboratory, 1991.

[20] V. Kumar and A. K. Datta. Vacuum ultraviolet scintillators: sodium salicylate and p-terphenyl. *Applied Optics*, 18(9):1416, 1979.